Breit-Pauli *R*-matrix method for electron-impact excitation to magnetic sublevels and x-ray-line polarization of ions

G. X. Chen

Harvard-Smithsonian Center for Astrophysics, 60 Garden Street, Cambridge, Massachusetts 02138, USA

(Received 18 November 2010; published 22 July 2011)

The Breit-Pauli *R*-matrix (BPRM) method was employed to calculate x-ray line polarization resulting from electron-impact excitation to excited-state magnetic sublevels (MS) of complex ions. In the development of this work, the calculation of MS electron-impact excitation cross sections in the present BPRM method is computationally efficient when the angular integration of the scattering polar angle is performed in an analytical manner. The BPRM method is then applied to calculate the line polarization of 3C ($\lambda = 15.01$ Å) and 3D ($\lambda = 15.26$ Å), two well-known x-ray lines of 17 (an ion with a medium nuclear charge and ion charge). We demonstrate in this work the resonance effects in MS cross sections, which contribute to the energy dependence in the polarization. The BPRM calculations of Fe XVII are further compared with the results calculated by the Dirac *R*-matrix (DRM) method. Generally, most of the results calculated from the BPRM method and the DRM method are in good agreement. This comparison confirms the earlier DRM calculations of resonance effects in MS electron-impact excitation cross sections of 3C and 3D, and thus demonstrates the applicability of the BPRM method to the calculation of x-ray line polarization of 3C and 3D, important for the analysis of x-ray spectra observed on an electron beam ion trap.

DOI: 10.1103/PhysRevA.84.012705 PACS number(s): 34.80.Dp, 32.30.Rj, 34.80.Nz

I. INTRODUCTION

The study of x-ray line polarization is needed for the physical interpretation and analysis of x-ray radiation spectrum in electron beam ion trap (EBIT) measurements [1,2]. An EBIT is a most useful devices for testing theoretical calculations of x-ray physics in highly charged, collisionally ionized plasmas [3,4]. In EBIT experiments, ions are excited by collisions with a beam of electrons, and the anisotropy of the beam's velocity distribution generally gives rise to excited states that can emit polarized lines. The polarization spectroscopic analysis may also provide new diagnostic insights for other laboratory and distant astrophysical plasmas. For example, x-ray line polarization spectroscopy may be applied to the future studies of plasma conditions and parameters of laser or Z-pinch inertial confinement fusion, magnetic confinement fusion, solar flares, coronal mass ejection, and other exotic sources [5–8].

The determination of the polarization of 3C and 3D lines in Fe XVII, an ion with a medium nuclear charge Z and ion charge z, has become essential for benchmarking theoretical calculations using an EBIT setup [2–4,9]. Lines 3C ($\lambda = 15.01$ Å) and 3D ($\lambda = 15.26$ Å) are two of the strongest Fe XVII x-ray lines, arising from dipole transitions $3d \rightarrow 2p$ with target state total angular momentum $J_t = 1^\circ \rightarrow 0$. Currently, a polarization value of 0.40, constant over a broad energy range for both the 3C and 3D lines has been used in the spectral analysis of EBIT experiments [3,10].

The relativistic close coupling Breit-Pauli *R*-matrix (BPRM) method has been extended to the calculations of magnetic sublevel (MS) electron impact excitation (EIE) cross sections for ions [11] and for neutral atoms [12]. The BPRM method was applied to the calculation of line polarization in He-like ions [11]. However, the BPRM method has not been applied to the calculation of MS EIE cross sections and polarization of Fe XVII. We note that the fully relativistic distorted-wave (RDW) method has been applied to the calculation of MS EIE cross sections and polarization of Fe XVII [13,14].

In our previous work [13], the fully relativistic Dirac *R*-matrix (DRM) method was extended to the calculations of MS EIE cross sections and line polarization for ions. This DRM method has also been applied to the calculation of MS EIE cross sections and x-ray line polarization of Fe XVII. It was found in Ref. [13] that polarization is a function of both the electron energy *and* the electron beam width. Therefore, a proper treatment of polarization is necessary for EBIT spectral analysis. Note that, in our 2009 PRA paper [13], there was an error in the computer code of the subroutine to calculate the Coulomb phase shift. Due to this error, the part of the numerical data in this paper to support our DRM method is incorrect (see the Comment and Reply in Ref. [13] for further discussion). However, the revised calculation in our 2010 Reply shows that the wealth of resonance features still appears to be real, and these features are reconfirmed by that revised calculation.

In this paper, we apply the BPRM method to calculate MS EIE cross sections and polarization of x-ray lines 3C and 3D of Fe XVII. The angular integration of the scattering polar angle in the expression of MS EIE cross section is performed analytically, so the calculation in the present BPRM method is computationally efficient. This technique is used here following the work of the distorted-wave (DW) method in Ref. [15] for the calculation of MS EIE of ions. This similar technique was also used in our previous development of the fully relativistic DRM method for the calculation of MS cross sections and x-ray line polarization.

We also carry out a comparative study of MS EIE cross sections and polarization of 3C and 3D of Fe XVII calculated by the BPRM method in this work and by the DRM method in our previous work. To our knowledge, a comparative study of MS EIE cross sections with the BPRM method and the DRM method has not been made in the literature. We note that a comparative study of EIE for fine-structure levels of Fe XVII

 ©2011 American Physical Society

by the BPRM calculation [16] and by the DRM calculation has been made in Ref. [17].

Following the Introduction, we outline the BPRM method for the calculation of MS EIE cross sections and x-ray line polarization of ions in Sec. II. In Sec. III, as a test case study, our BPRM method is employed to the calculation of MS EIE cross sections and x-ray line polarization of Fe XVII. The BPRM calculations are compared with the results calculated by the DRM method. A brief summary and discussion is given in Sec. IV.

II. THEORY

Here we sketch the relevant details of the two main aspects in the BPRM theory: the relativistic calculations and the nature of electron correlation effects or channel coupling effects in the close coupling (CC) expansion. In the BPRM theory, the Hamiltonian is given as follows [18]:

$$H_{N+1}^{\rm BP} = H_{N+1}^{\rm NR} + H_{N+1}^{\rm mass} + H_{N+1}^{\rm Dar} + H_{N+1}^{\rm so}. \qquad (2.1)$$

In this equation $H_{N+1}^{\rm NR}$ is the nonrelativistic Hamiltonian along with the one-body mass-velocity term, the Darwin term, and the spin-orbit term—the result of reducing the Dirac equation to the Pauli form and dropping two-body electron-electron contributions. Since only the last terms breaks LS symmetry (leading to fine-structure levels $J\pi$ of total angular momentum quantum number J at parity π), mass and Darwin terms may be retained to great effect in computationally cheaper LS coupling calculations.

Relativistic fine-structure transitions in the Breit-Pauli approximation may be considered with an intermediate JK pair-coupling representation:

$$\vec{J}_\iota + \vec{\ell}_\iota = \vec{K},$$
$$\vec{K} + \vec{s}_\iota = \vec{J}, \qquad (2.2)$$

where $\vec{\ell}_\iota$ and $\vec{s}_\iota$ are the orbital and spin angular momentum of the free electron, respectively. The total angular momentum J_ι refers to the target level.

Using a partial wave expansion for the colliding electron in the BPRM method, the coupled-channel wave function in the inner region for the (e + Fe XVII) system at a given symmetry $J\pi$ (in an intermediate pair-coupling scheme) may be expressed as products of the target ion states and partial waves:

$$\Psi(E;{\rm e}+{\rm Fe\,XVII}) = \sum_i \chi_i({\rm Fe\,XVII})\theta_i(\ell) + \sum_j c_j \Phi_j({\rm Fe\,XVI}), \qquad (2.3)$$

where Ψ denotes the continuum ($E > 0$) states of a given symmetry $J\pi$, expanded in terms of the core ion eigenfunctions χ_i(Fe XVII) with a specific total angular momentum and parity combination $J_\iota\pi_\iota$, and the ℓ_ι partial wave $\theta_i(\ell_\iota)$ (containing radial bases) for the colliding $(N+1)$th electron with wave number k_ι in a channel labeled $J_\iota\pi_\iota\ k_\iota\ell_\iota[J\pi]$ (the channel energy $k_\iota^2 < 0$ if the channel is closed). The symbol Φ_j(Fe XVI) marks correlation wave functions made up of $(N+1)$ bound electrons to (a) compensate for the orthogonality conditions imposed on continuum with bound orbitals and (b) represent additional short-range correlations that are often of crucial importance in scattering and radiative CC calculations. The variationally added functions Φ_j(Fe XVI), sometimes referred to as "bound channels" as opposed to the continuum or "free" channels in the first sum over the target states, form a set of L^2-integrable antisymmetrized wave functions. The BPRM method is used to find the unknown continuum radial functions $\theta_i(\ell)$ and CC expansion coefficients c_j in Eq. (2.3). The continuum states satisfy certain boundary conditions. In Eq. (2.3), both spectroscopic orbitals and pseudo-orbitals may be included.

In relativistic BPRM calculations, sets of collisional symmetry $SL\pi$ are recoupled to obtain the states of the (e + Fe XVII) system with total $J\pi$, followed by diagonalization of the $(N+1)$-electron Hamiltonian. Details of diagonalizing $H_{N+1}^{\rm BP}$ at the R-matrix boundary are given in Ref. [19], as is the outward propagation.

The reactance **K**-matrix describes the asymptotic form of the entire wave function of the (e + Fe XVII) system for the scattering process. In BPRM theory, when matching the inner and outer regions, the **K**-matrix may be obtained from a set of asymptotic radial functions for the open channels,

$$F_{ii'}(r) \longrightarrow k_i^{-1/2}(\sin\varphi_i\delta_{ii'} + \cos\varphi_i K_{ii'}) \quad \text{when } r \to \infty, \qquad (2.4)$$

$$\varphi_i = k_i r - \tfrac{1}{2}\ell_i\pi + \eta_i \ln(2k_i r) + \sigma_{\ell_i}, \qquad (2.5)$$

where $\eta_i = (Z-N)/k_i$ and i' indexes the linearly independent solution of the coupled equations in the outer region. The Coulomb phase shift σ_{ℓ_i} for the orbital angular momentum ℓ_i of the free electron is given by

$$\sigma_{\ell_i} = \arg\Gamma(\ell_i + 1 - {\rm i}\eta_i). \qquad (2.6)$$

When the electron is scattered from direction $\hat{\mathbf{k}}_i$ to $\hat{\mathbf{k}}_f$, the scattering amplitude (with the Condon-Shortley phase convention for the spherical harmonics) $f(\alpha_i J_i M_i, \alpha_f J_f M_f)$ from the initial sublevel $\alpha_i J_i M_i$ to the final sublevel $\alpha_f J_f M_f$ of the target is expressed in terms of the **T**-matrix by [13,15,20]

$$f(\alpha_i J_i M_i, \alpha_f J_f M_f) = \frac{2\pi}{\sqrt{k_i k_f}} \sum_{\ell_i m_{\ell_i}} \sum_{\ell_f m_{\ell_f}} {\rm i}^{\ell_i - \ell_f + 1} {\rm e}^{{\rm i}(\sigma_{\ell_i} + \sigma_{\ell_f})} \times Y^*_{\ell_i m_{\ell_i}}(\hat{\mathbf{k}}_i) Y_{\ell_f m_{\ell_f}}(\hat{\mathbf{k}}_f) T_{\beta_i \beta_f}, \qquad (2.7)$$

where the symbols C and Y are Clebsch-Gordan coefficients and spherical harmonics, respectively; and the symbols M and m are the corresponding magnetic quantum numbers. The notation $\beta_i = \ell_i 1/2 m_{\ell_i} m_{s_i} \alpha_i J_i M_i$ and $\beta_f = \ell_f 1/2 m_{\ell_f} m_{s_f} \alpha_f J_f M_f$ with α_i and α_f the additional quantum numbers is used to specify the initial and final target magnetic states, respectively.

The expression of MS EIE cross section $\sigma(\alpha_i J_i M_i, \alpha_f J_f M_f)$ is then given by

$$\sigma(\alpha_i J_i M_i, \alpha_f J_f M_f) = \frac{k_f}{2k_i} \int \sum_{m_{s_i}} \sum_{m_{s_f}} |f(\alpha_i J_i M_i, \alpha_f J_f M_f)|^2 d\hat{\mathbf{k}}_f. \qquad (2.8)$$

In order to obtain a computationally efficient expression for $\sigma(\alpha_i J_i M_i, \alpha_f J_f M_f)$, we perform an analytical angular integration for Eq. (2.8), with the aid of the orthogonality

of spherical harmonics, following the development of the DW method in Ref. [15]. After transforming the **T**-matrix from the uncoupled representation to the coupled representation,

$$T_{\beta_i\beta_f} = \sum_{JM}\sum_{K_iM_{K_i}}\sum_{K_fM_{K_f}} C^{J_i\ell_iK_i}_{M_im_{\ell_i}M_{K_i}} C^{K_i1/2J}_{M_{K_i}m_{s_i}M} \times C^{J_f\ell_fK_f}_{M_fm_{\ell_f}M_{K_f}} C^{K_f1/2J}_{M_{K_f}m_{s_f}M} T_{\gamma_i\gamma_f}, \quad (2.9)$$

we derive the final analytical expression for MS EIE cross section $\sigma(\alpha_iJ_iM_i,\alpha_fJ_fM_f)$ (in units of πa_0^2 with a_0 as the Bohr radius):

$$\sigma(\alpha_iJ_iM_i,\alpha_fJ_fM_f) = \frac{1}{2k_i^2}\sum_{JJ'}\sum_{\ell_i\ell_i'}\sum_{K_iK_i'}\sum_{K_fK_f'}\sum_{\ell_f}\sum_{m_{s_i}}\sum_{m_{s_f}} \times \mathrm{i}^{\ell_i-\ell_i'}[(2\ell_i+1)(2\ell_i'+1)]^{\frac{1}{2}}\mathrm{e}^{\mathrm{i}(\sigma_{\ell_i}-\sigma_{\ell_i'})} \times C^{J_i\ell_iK_i}_{M_i0M_i} C^{K_i1/2J}_{M_im_{s_i}M} C^{J_f\ell_fK_f}_{M_fm_{\ell_f}M_{K_f}} C^{K_f1/2J}_{M_{K_f}m_{s_f}M} C^{J_i\ell_i'K_i'}_{M_i0M_i} C^{K_i'1/2J'}_{M_im_{s_i}M} \times C^{J_f\ell_fK_f'}_{M_fm_{\ell_f}M_{K_f}} C^{K_f'1/2J'}_{M_{K_f}m_{s_f}M} T_{\gamma_i\gamma_f} T^*_{\gamma_i'\gamma_f'}. \quad (2.10)$$

Here $\gamma_i = J_i\ell_iK_i1/2\ \alpha_iJM$ and $\gamma_f = J_f\ell_fK_f1/2\ \alpha_fJM$. The factor $\mathrm{i}^{\ell_i-\ell_i'}$ on the RHS of Eq. (2.10) should be removed if the Fano and Racah phase convention instead of the Condon-Shortley phase convention for the spherical harmonics is adopted. The unitarized and complex **T**-matrix is calculated from the symmetric **K**-matrix by

$$\mathbf{T} = 2\mathrm{i}\mathbf{K}/(\mathbf{I} - \mathrm{i}\mathbf{K}). \quad (2.11)$$

The **K**-matrix calculated by the BPRM codes [19] provides the input to the computer program for the calculation of MS EIE cross sections.

III. CALCULATION AND RESULTS

We have written a computer program, based upon the formulas of the BPRM method developed in the preceding section, to calculate the specific MS EIE cross sections $\sigma_0(E)$ and $\sigma_1(E)$ for both 3C and 3D of Fe XVII. We use the notation $\sigma_0(E)$ and $\sigma_1(E)$ to represent MS EIE cross sections with the magnetic quantum number of the upper-level $M_f = 0$ and $M_f = 1$, respectively. The computer program is then used to calculate the polarization of 3C and 3D x-ray line emission in Fe XVII.

In our BPRM calculations, we constructed a large eigenfunction expansion over the 15 configurations $2s^22p^6$, $2s^22p^5n\ell$, $2s2p^6n\ell$ up to the principal quantum number $n = 3$ and the $n = 4$ complexes of Fe XVII, yielding 89 fine-structure *levels* corresponding to 49 *LS terms*. Full details of the target calculations and the BPRM calculation for EIE cross sections between fine-structure levels have been reported in our previous work [9,16].

The effective EIE cross section $\bar{\sigma}(E,W)$ is defined from the detailed MS excitation cross section $\sigma(E')$ as

$$\bar{\sigma}(E,W) = \frac{\int \sigma(E')g(E,W;E')v_\mathrm{e}dE'}{\int g(E,W;E')v_\mathrm{e}dE'}, \quad (3.1)$$

where v_e is the velocity of the incident electron. The electron distribution function is $g(E,W;E')$ and, for an EBIT, is generally assumed to be a Gaussian peaked at E, with a full width at half maximum defined as W.

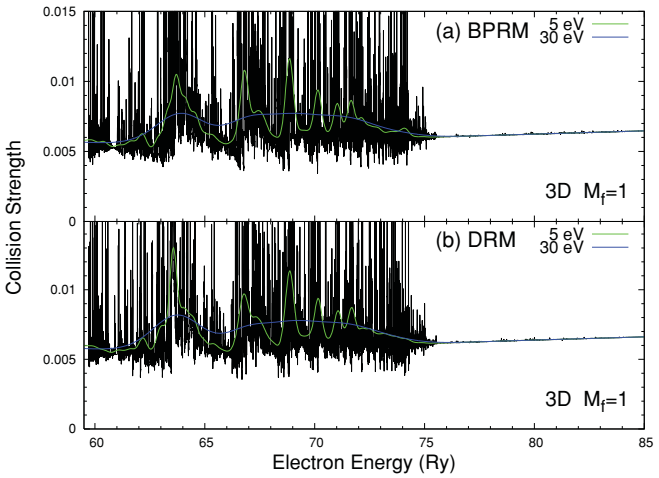

FIG. 1. (Color online) Collision strength Ω (black) and effective collision strengths $\bar{\Omega}$ (colored or gray curves) for EIE to 3D magnetic sublevel $M_f = 1$ of Fe XVII: (a) BPRM method, (b) DRM method. Green (gray with oscillation) curve: $W = 5$ eV; blue (gray without oscillation) curve: $W = 30$ eV.

Figures 1 and 2 show the MS collision strengths $\Omega = w_ik_i^2\sigma$ as a function of incident electron energy E_i for 3D, where w_i is the statistical weight of the initial state and k_i is the wave number of the incident electron. The effective MS collision strengths $\bar{\Omega}$ for $W = 5$ eV and $W = 30$ eV are also shown in the figures to gauge the resonance effects. The BPRM calculation is shown in the upper panel, and the DRM calculation is shown in the lower panel for comparisons. Large resonance effects and complicated resonance structures are demonstrated in both Figs. 1 and 2. In the low-energy resonance region, the effect of resonances may enhance the background collision strengths by an amount up to as much as 40% or more, depending on the electron energy and the beam width. The features of 3D collision strengths calculated by the BPRM and DRM methods are generally in good agreement, except for the case of $\bar{\Omega}$ with a smaller $W = 5$ eV, for which we find some significant differences. We note that the backgrounds of the 3D MS collision strengths in this work are in agreement with the previous RDW calculations with the inclusion of the target states up to $n = 3$ [14]. In the energy range shown in our figures, the MS collision strengths from this RDW calculation for 3D are 5.58×10^{-3} at $E_i = 62.78$ Ry and 6.10×10^{-3} at $E_i = 74.78$ Ry for $M_\mathrm{f} = 1$; and 1.22×10^{-2} at $E_i = 62.78$ Ry and 1.46×10^{-2} at $E_i = 74.78$ Ry for $M_\mathrm{f} = 0$, respectively.

Similarly, Figs. 3 and 4 show the detailed and effective MS collision strengths as a function of incident electron energy E_i for 3C. Again, the background collision strengths and resonance features calculated by the BPRM method and the DRM method are generally in good agreement. As seen from Figs. 3 and 4, resonance effects are also a bit significant for 3C, although they are less strong than for the case of 3D. This is expected, because 3D is an intercombination dipole transition while 3C is not. We note that the backgrounds of the 3C MS collision strengths in this work are also in agreement

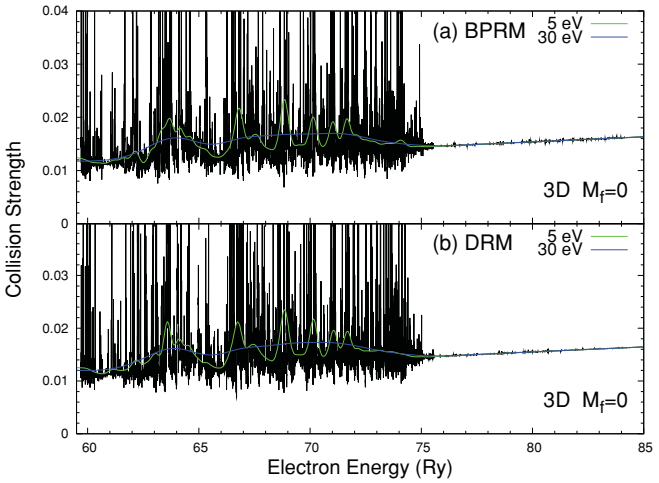

FIG. 2. (Color online) Collision strength Ω (black) and effective collision strengths $\bar{\Omega}$ (colored or gray curves) for EIE to 3D magnetic sublevel $M_f = 0$ of Fe XVII: (a) BPRM method; (b) DRM method. Green (gray with oscillation) curve: $W = 5$ eV; blue (gray without oscillation) curve: $W = 30$ eV.

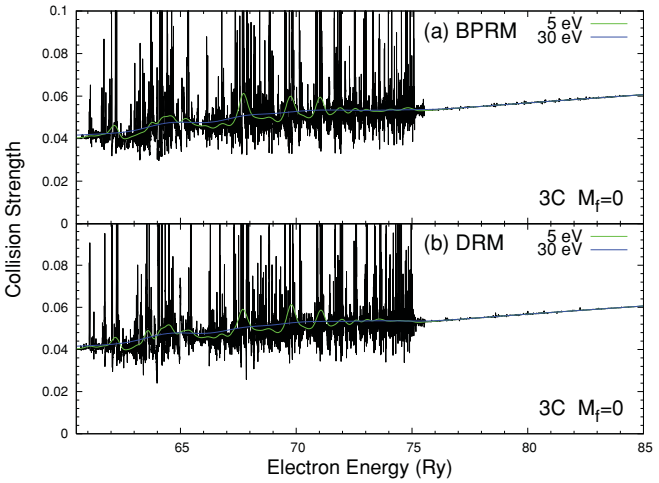

FIG. 4. (Color online) Collision strength Ω (black) and effective collision strengths $\bar{\Omega}$ (colored or gray curves) for EIE to 3C magnetic sublevel $M_f = 0$ of Fe XVII: (a) BPRM method; (b) DRM method. Green (gray with oscillation) curve: $W = 5$ eV; blue (gray without oscillation) curve: $W = 30$ eV.

with the previous RDW calculations with the inclusion of the target states up to $n = 3$ [14]. In the energy range shown in our figures, the MS collision strengths from this RDW calculation for 3C are 2.14×10^{-2} at $E_i = 63.82$ Ry and 2.39×10^{-2} at $E_i = 75.82$ Ry for $M_f = 1$; and 4.65×10^{-2} at $E_i = 63.82$ Ry and 5.66×10^{-2} at $E_i = 75.82$ Ry for $M_f = 0$, respectively.

When the 3C and 3D x-ray emission is observed at an angle of 90° with respect to the electron beam direction in EBIT measurements, the polarization can be calculated from the MS EIE cross sections $\sigma_0(E)$ and $\sigma_1(E)$ [20]. The energy-dependent expression of polarization $P(E)$ for 3C and 3D is defined as [13]

$$P(E) = \frac{\sigma_0(E) - \sigma_1(E)}{\sigma_0(E) + \sigma_1(E)}. \tag{3.2}$$

Further detailed discussions for the degree of linear polarization of the emitted radiation are given in our previous paper [13].

Our polarization calculations for 3C and 3D are shown in Figs. 5 and 6. Generally, the polarization calculated with the BPRM and DRM methods are in good agreement, except for the case of $\bar{P}(E,W)$ with a smaller $W = 5$ eV, for which we find noticeable differences. The polarization of 3C and 3D is shown in the figures to be energy dependent, in particular in the resonance region with low incident electron energy. Furthermore, oscillation features in polarization are more pronounced in 3D. Due mainly to the resonances in MS cross sections, negative polarization at certain energy regions show up in both 3C and 3D.

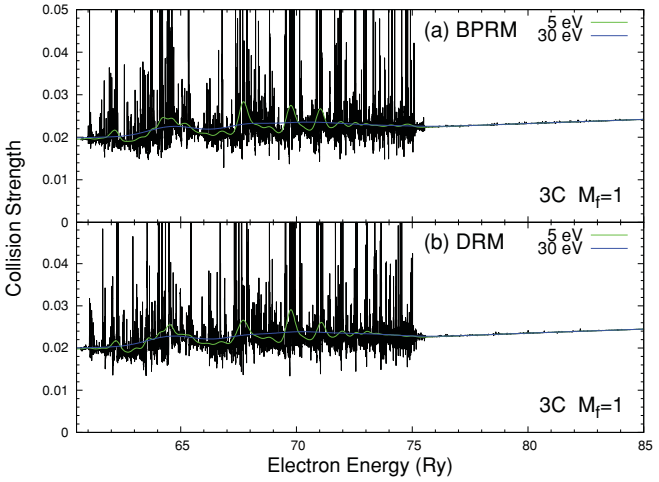

FIG. 3. (Color online) Collision strength Ω (black) and effective collision strengths $\bar{\Omega}$ (colored or gray curves) for EIE to 3C magnetic sublevel $M_f = 1$ of Fe XVII: (a) BPRM method; (b) DRM method. Green (gray with oscillation) curve: $W = 5$ eV; blue (gray without oscillation) curve: $W = 30$ eV.

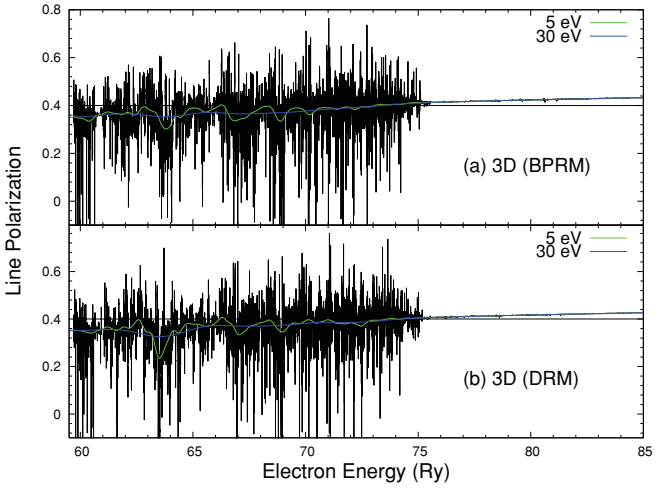

FIG. 5. (Color online) Polarization $P(E)$ (black) and effective polarization $\bar{P}(E,W)$ (green or gray curve with oscillation for $W = 5$ eV; blue or gray curve without oscillation for $W = 30$ eV) in 3D of Fe XVII. Top panel: BPRM method; bottom panel: DRM method. Dotted curve: a constant value used in EBIT [3,10].

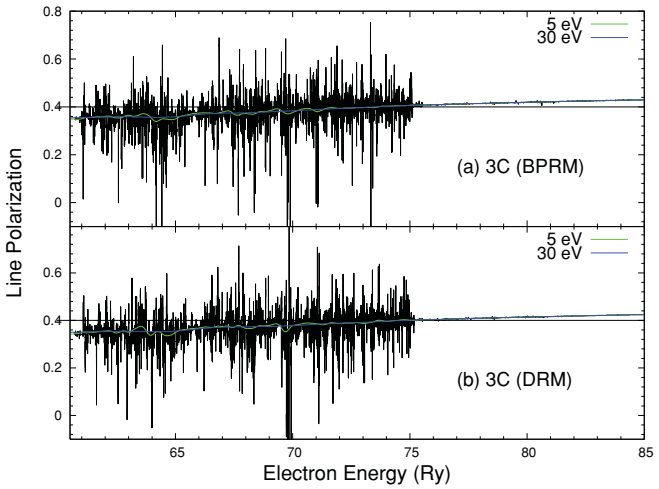

FIG. 6. (Color online) Polarization $P(E)$ (black) and effective polarization $\bar{P}(E,W)$ (green or gray curve with oscillation for $W =$ 5 eV; blue or gray curve without oscillation for $W = 30$ eV) in 3C of Fe XVII. Top panel: BPRM method; bottom panel: DRM method. Dotted curve: a constant value used in EBIT [3,10].

The effective polarization $\bar{P}$ is defined as [13]

$$\bar{P}(E,W) = \frac{\bar{\sigma}_0(E,W) - \bar{\sigma}_1(E,W)}{\bar{\sigma}_0(E,W) + \bar{\sigma}_1(E,W)}. \tag{3.3}$$

The effective polarization $\bar{P}$ calculated using Eq. (3.3) is also shown in Figs. 5 and 6. For 3C, $\bar{P}$ varies little for both $W = 5$ and 30 eV, but for 3D, $\bar{P}$ shows large oscillations in E. Depending on the electron beam energy and the beam width, the effective polarization of 3C and 3D may significantly deviate the constant value of 0.4, which is currently used in the analysis of EBIT x-ray spectrum [3,10]. We note that cascade effects may not play an important role for the polarization calculations at low energy, and they are not included in the present calculations.

IV. SUMMARY AND DISCUSSION

In this work, we report a BPRM method and develop a computer program to calculate EIE to magnetic sublevels and x-ray line polarization. The BPRM method is applied to the calculations of EIE to specific MS of the upper states of the 3C and 3D transitions in Fe XVII, from which we compute the line polarizations. The present BPRM method is computationally efficient when the angular integration of the scattering polar angle is performed analytically. From the results of our BPRM calculations, resonance effects in MS EIE cross sections and oscillation features in polarization are demonstrated.

We also report the corresponding calculations from our DRM method [13] for comparisons. For a specific case study of MS EIE for strong dipole lines 3C and 3D of Fe XVII, which is an ion with a medium nuclear charge Z and medium ionization state (i.e., with a medium ion charge z), a generally good agreement for most of the results calculated from the BPRM method and the DRM method is established in this work. This agreement shows the applicability of the BPRM method to the calculation of x-ray line polarization of 3C and 3D, important for the analysis of EBIT x-ray line spectrum. We should note that this agreement may be expected only where the applications of the BPRM and DRM methods overlap. Because the BPRM method is generally computationally more efficient than the DRM method, one may further argue that the BPRM method for the calculations of the MS cross sections and polarization (of strong dipole lines in particular) is more applicable to ions with a low to medium nuclear charge Z and ion charge z, while the DRM method is more applicable to ions with a medium to high nuclear charge Z or ion charge z.

ACKNOWLEDGMENTS

This work was supported in part by a grant from Smithsonian Astrophysical Observatory (SAO) and by NASA to SAO for the Chandra X-ray Center through grants TM0-11001X and TM8-9001X.

[1] J. N. Tan, E. Silver, J. Pomeroy, J. M. Laming, and J. Gillaspy, Phys. Scr. T **119**, 30 (2005).
[2] G. X. Chen, K. Kirby, E. Silver, N. S. Brickhouse, J. D. Gillaspy, J. N. Tan, J. M. Pomeroy, and J. M. Laming, Phys. Rev. Lett. **97**, 143201 (2006).
[3] G. V. Brown, P. Beiersdorfer, D. A. Liedahl, and K. Widmann, Astrophys. J. **502**, 1015 (1998).
[4] J. M. Laming *et al.*, Astrophys. J. **545**, L161 (2000); J. D. Gillaspy *et al.*, *ibid.* **728**, 132 (2011).
[5] J. C. Kieffer, J. P. Matte, H. Pepin, M. Chaker, Y. Beaudoin, T. W. Johnston, C. Y. Chien, S. Coe, G. Mourou, and J. Dubau, Phys. Rev. Lett. **68**, 480 (1992).
[6] T. Kawamura, T. Kai, F. Koike, S. Nakazaki, Y. Inubushi, and H. Nishimura, Phys. Rev. Lett. **99**, 115003 (2007).
[7] T. Fujimoto, H. Sahara, T. Kawachi, T. Kallstenius, M. Goto, H. Kawase, T. Furukubo, T. Maekawa, and Y. Terumichi, Phys. Rev. E **54**, R2240 (1996); A. S. Shlyaptseva *et al.*, Rev. Sci. Instrum. **72**, 1241 (2001).
[8] E. Haug, Sol. Phys. **61**, 129 (1979); J. M. Laming, Astrophys. J. **357**, 275 (1990).
[9] G. X. Chen and A. K. Pradhan, Phys. Rev. Lett. **89**, 013202 (2002); G. X. Chen, Phys. Rev. A **76**, 062708 (2007).
[10] G. V. Brown *et al.*, Phys. Rev. Lett. **96**, 253201 (2006).
[11] T. Kai, S. Nakazaki, T. Kawamura, H. Nishimura, and K. Mima, Phys. Rev. A **75**, 012703 (2007).
[12] A. N. Grum-Grzhimailo, Comput. Phys. Commun. **152**, 101 (2003).
[13] G. X. Chen, K. Kirby, N. S. Brickhouse, T. Lin, and E. Silver, Phys. Rev. A **79**, 062715 (2009); **82**, 036702 (2010); H. L. Zhang, C. J. Fontes, and C. P. Ballance, *ibid.* **82**, 036701 (2010). There are also several typographical errors in our 2009 Phys. Rev. A paper: in Eq. (3.7), the factor $\frac{2}{k_i^2}$ should be replaced by $\frac{1}{2k_i^2}$ and $\sigma_{\ell'_f}$ should be replaced by $\sigma_{\ell'_i}$; in Eqs. (3.5) and (3.6), k_j should be replaced by k_f.

[14] H. L. Zhang, D. H. Sampson, and R. E. H. Clark, Phys. Rev. A **41**, 198 (1990).

[15] M. K. Inal and J. Dubau, J. Phys. B **20**, 4221 (1987); **22**, 3329 (1989).

[16] G. X. Chen, A. K. Pradhan, and W. Eissner, J. Phys. B **36**, 453 (2003).

[17] S. D. Loch, M. S. Pindzola, C. P. Ballance, and D. C. Griffin, J. Phys. B **39**, 85 (2006).

[18] N. S. Scott and K. T. Taylor, Comput. Phys. Commun. **25**, 347 (1982).

[19] K. A. Berrington, W. Eissner, and P. H. Norrington, Comput. Phys. Commun. **92**, 290 (1995). The updated BPRM codes are given at [http://amdpp.phys.strath.ac.uk/UK_RmaX/codes.html].

[20] I. C. Percival and M. J. Seaton, Philos. Trans. R. Soc. London A **251**, 113 (1958).